

LA-UR-

Approved for public release;
distribution is unlimited.

08-63941

Title: Large temporal window contrast measurement using optical parametric amplification and low-sensitivity detectors

Author(s): Rahul C. Shah, Randall P. Johnson, Tsutomu Shimada, and B. M. Hegelich

Intended for: European Journal of Physics D



Los Alamos National Laboratory, an affirmative action/equal opportunity employer, is operated by the Los Alamos National Security, LLC for the National Nuclear Security Administration of the U.S. Department of Energy under contract DE-AC52-06NA25396. By acceptance of this article, the publisher recognizes that the U.S. Government retains a nonexclusive, royalty-free license to publish or reproduce the published form of this contribution, or to allow others to do so, for U.S. Government purposes. Los Alamos National Laboratory requests that the publisher identify this article as work performed under the auspices of the U.S. Department of Energy. Los Alamos National Laboratory strongly supports academic freedom and a researcher's right to publish; as an institution, however, the Laboratory does not endorse the viewpoint of a publication or guarantee its technical correctness.

Large temporal window contrast measurement using optical parametric amplification and low-sensitivity detectors

Rahul C. Shah, Randall P. Johnson, Tsutomu Shimada, and B. M. Hegelich

Los Alamos National Laboratory, Los Alamos, NM 87545, USA

Received: date / Revised version: date

Abstract. To address few-shot pulse contrast measurement, we present a correlator coupling the high gain of an optical parametric amplification scheme with large pulse tilt. This combination enables a low sensitivity charge coupled device (CCD) to observe features in the pulse intensity within a 50 ps single-shot window with inter-window dynamic range $> 10^7$ and < 0.5 mJ input energy. Partitioning of the single window with optical densities to boost the CCD dynamic range is considered.

PACS. 42.60.Jf Laser beam characteristics: profile, intensity, and power; spatial pattern formation – 42.65.Yj Optical parametric oscillators and amplifiers – 52.38.Kd Laser-plasma acceleration of electrons and ions

1 Introduction

Quality of the laser-matter interaction at terawatt powers achieved with sub-ps pulses depends on premature target ionization by preceding intensity spikes or amplified spontaneous emission (ASE). As a specific example, the threshold for destruction of \sim nm target foils in laser-based ion acceleration schemes [1] occurs at 10^{10} W/cm 2 . At typical peak interaction intensities of $\sim 10^{20}$ W/cm 2 , this translates to a requirement of better than 10^{-10} intensity contrast a few ps from the peak. This requirement climbs to 10^{-15} for the planned Extreme Light Infrastructure [2] at an intensity $\sim 10^{25}$ W/cm 2 . Systems providing the required energies and intensities often fire only few times per hour so scanning contrast measurements can be made only as far as lower mJ amplification states. This should suffice to establish ASE levels but concern exists over compression quality [3] and pre-pulse production from reflections due to non-linearity [4]. Scanning contrast measurements most commonly use sum frequency generation between the doubled and fundamental light to remove competing optical background and obtain high-dynamic range. Most recently fabry-perot etalons were used to create second harmonic pulses of variable intensities delayed in intervals of 40 ps allowing single shot dynamic range of $> 10^6$ over 200 ps with an 8-bit CCD [5]. Mixing the beams at an angle to delay one pulse front with respect to the other across the resulting beam presents another approach [6]. With the pulse front simply perpendicular to the propagation, the walk-off of the mixing beams and phase-matching requirements limit the angle and temporal window. Use of angular dispersion from a grating can dramatically in-

crease pulse tilt to order 200 ps/cm, and a three window measure spanned 100 ps with dynamic range approaching 10^6 [7]. Also recently, use of a wedge to create attenuated replicas of the output allowed a non-blooming 8-bit CMOS to obtain a single shot trace of 10^4 dynamic over 20 ps using 0.1 mJ [8].

Sum-frequency generation limits the amount of detectable energy to that contained in the measured time-slice of the input. Optical parametric amplification (OPA) forms a separate class of correlator (OPAC) whereby the doubled light acts as pump to amplify the fundamental [9]. This can allow measurement of more extreme contrasts with given input energy. OPA produces a duplicate of only the amplified time-slice in a third wave known as the idler, and with non-collinear geometry, it separates spatially. Competing background comes from either scattering of the degenerate signal or optical parametric noise (OPN). In the previously demonstrated scanning configuration with mJ input the gain reached 10^6 giving $> 10^{11}$ dynamic range with a silicon photodiode. A demonstrated single shot implementation of this scheme considered only a large difference in propagation angle to create the temporal window and 8-bit dynamic range [3]. In this work, we use pulse tilt coupled with OPAC to obtain 50 ps window with inter-window dynamic range of $> 10^7$. Unique considerations in signal-to-noise for few/single shot geometry are identified. To improve the dynamic range of the detector we consider the use of a set of metal absorbing layers on glass slides to partition the temporal window to different intensity levels. The analysis indicates paths towards improvement of both inter- and intra-windows dynamic ranges.

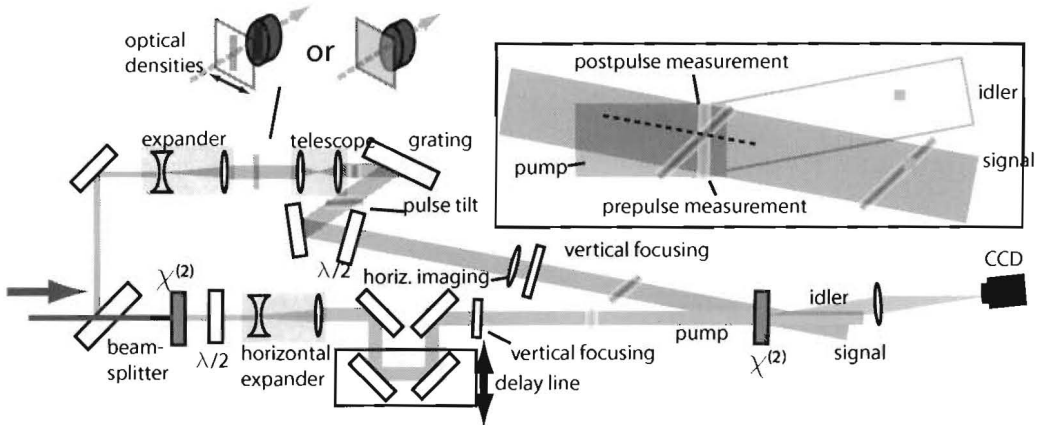


Fig. 1. Schematic arrangement of large temporal window pulse contrast measurement based on optical parametric amplification. Inset shows zoom of the final mixing illustrating how the tilted signal wavefront results in amplification of varied delays. SHAHsetup-fig1.eps.

2 Specific Considerations

The inset of Fig. 1 concisely summarizes the concept of the correlator. The pump (green), formed by doubling a portion of the available beam, amplifies the input signal. In the scanning geometry pulse tilt acts to compensate the non-collinear angle so as to amplify across the entire pulse front. Here the tilt creates a wide range of signal delays over which the pump acts. The interesting advantage of the OPAC comes from the exponential gain G of the signal and idler given by $G = e^{g z} / 4$ [10] where, with BBO crystal and $\lambda = 1 \mu\text{m}$, $g = 2.7 \times 10^{-5} \sqrt{I} [\text{W/cm}^2] z [\text{mm}]$. With pump energy of $100 \mu\text{J}$, duration 500 fs and line focus $1 \text{ cm} \times 50 \mu\text{m}$ the gain exceeds 10^4 with $z=2 \text{ mm}$. Because of the square root dependence on I , 10% stability of the pump between temporal windows limits gain fluctuation within a factor of two. Likewise using pump beam width twice that imposed by the desired single-shot temporal span applies this criteria to the intra-window gain profile.

The large angular tilt between pulse fronts ($\sim 70^\circ$), coupled with small non-collinear propagation angle between pump and signal (5°) that laterally separates the signal and idler, lead to several unique considerations. This spatial walk-off maps to temporal resolution: the lateral spread after 2 mm (crystal length) gives $\sim 4 \text{ ps}$. The influences on the gain also seem reasonable. For a laser signal of $150 \mu\text{m}$ coherence length, the walk-off occurs over 0.5 mm in the propagation direction. Numerically solving the coupled equations with an exponential decay term acting on idler amplitude shows a $6\times$ reduction. Because of the pulse tilt, contributions from neighboring delays become incoherent for even shorter propagation lengths. Calculation of group velocity mismatch shows minimal influence on the total gain for these durations and angles.

OPN limits the smallest signal which can be measured. One can interpret it as resulting from amplification of 1 photon per mode per unit frequency [11], and barring other noise sources, the ratio with per mode input power gives maximum measurable contrast. In the scanning scheme [9], the pump amplified an entire Gaussian

signal beam clearly defining this as the system mode. In a single shot scheme, the pump amplifies small spatial slices which a lens images to the CCD. The number of modes more closely pertains to the diffraction limit of the final imaging system (which ideally should match the needed imaging resolution) [12]. Considering an input signal of $10 \mu\text{J}$ focused over $1 \text{ cm} \times 100 \mu\text{m}$, an $f/4$ lens, 10 nm bandpass, and realization of the maximum gain by the noise, the measurable contrast is $\sim 10^{-10}$. With regards to the OPN one can increase the measurable contrast by upping the input. A second limit on the contrast measurement is imposed by the scattering between the degenerate signal and idler beams. Again, imaging of the crystal exit as opposed to beam propagation makes the single shot configuration far more sensitive to this noise, and this turns out to be the principal limiting factor.

3 Experiment and Analysis

Referring to Fig. 1, 90% of the transform-limited, p-polarized, 500 fs , $200 \mu\text{J}$, $\lambda_0=1053 \text{ nm}$ pulse passes through the beam-splitter. A 2 mm , Type I BBO crystal generates $140 \mu\text{J}$ second harmonic. Since the pump eventually focuses tightly in the vertical direction, a waveplate rotates the polarization so as to have the Poynting vector walkoff in the horizontal plane. Cylindrical lenses expand the 3 mm beam in the horizontal dimension to $\sim 1 \text{ cm}$, and after a variable delay line with manual vernier, a 300 mm cylindrical lens focuses the beam to a second Type I BBO for the OPA. The signal beam is first expanded to 1 cm and then a telescope images it to a 1740 lines/mm grating. The telescope allows the introduction of spatially selective optical densities detailed subsequently. The angle between incident and exiting beams roughly measured 12° corresponding to a pulse tilt of 74° [13]. To preserve the pulse compression, a cylindrical lens images the grating plane to the final crystal. Mixing occurs at propagation angle of 5° with respect to the pump. Spectral clipping should induce coherent contrast effects at levels below our interest

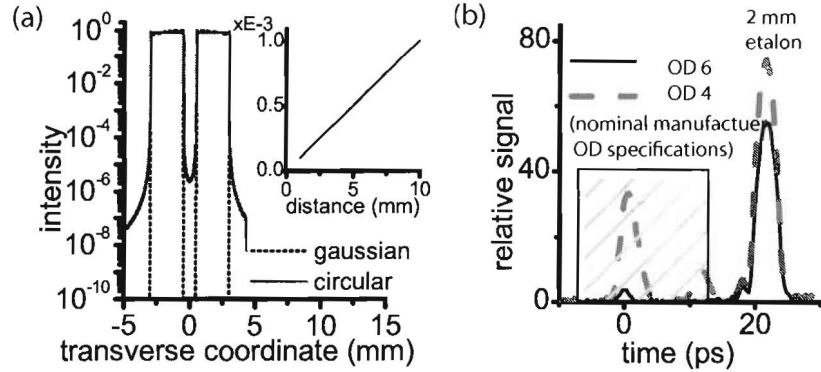


Fig. 2. (a) Calculated image for opaque 1 mm step for the cases of both hard (solid red) and Gaussian apertures (dotted black). Inset pertains to out-of-plane image blur and shows Fresnel knife-edge diffraction at 0.5 mm transverse distance from the step edge for increasing propagation lengths. Zero corresponds to image plane. (b) Single window measurement of principle peak and 10^{-3} etalon reflection. Optical densities are manufacturer neutral density specifications. Hatched region corresponds to 1 mm width of step densities. SHAhaptures-fig2.eps.

for this first prototype; eventually the pump could receive the pulse tilt instead. A separate cylindrical lens loosely focuses the signal in the vertical dimension. Idler beam and signal are imaged to unique CCDs. By using glass absorbing filters in the signal arm, the gain measures 10^4 consistent with the pump intensity. Varying the delay line shows a temporal delay across the beam of 200 ps/cm. This corresponds to pulse tilt of 80° in agreement with the above angles, and a window of about 3 mm shows uniform gain. With the pump blocked, the idler imaging measures scatter from the signal arm at a level $\sim 10^{-8}$ with respect to that of the pulse peak. Given the gain, this corresponds to scattering contribution of 10^{-4} , and for this reason, the signal beam is vertically focused only to ~ 1 mm on the crystal face. With the input signal blocked, the imaged OPN is at least 4x below the scatter (optical densities in front of the CCD brought it below the detection level). The intersection between OPN and scattering marks a limit on the achievable dynamic range of this implementation.

Between temporal windows, one easily selects the dynamic range by use of glass absorbing filters. To address the dynamic range within a temporal window, we have considered the use of glass slides with 1 mm wide metallic optical density (Bayview Optics, Dover-Foxcroft, ME). In our implementation, a telescope images the optical density to the grating plane, and while monitoring the idler image, it is slid to cover the desired temporal peak (Fig. 1). The nm-scale thickness of the absorber means that the entire beam experiences the same delay. A potential limit of this approach results directly from the diffractive properties of the coherent imaging system and the output electric field E can be calculated from the convolution[14]

$$E(x) \propto [g(-x) \exp\left(\frac{ikx^2}{2f}\right)] * \bar{P}(f_x = \frac{x}{\lambda f}) \quad (1)$$

where $g(x)$ is input electric field, $k = 2\pi/\lambda$, and \bar{P} is the Fourier transform of the lens aperture. Fig. 2(a) shows the numerical result of the convolution for a 1 mm opaque step

at beam center for both hard ($f/6$) and Gaussian (full-width-half-maximum (FWHM)) apertures. For the hard aperture the sinc function limits the image contrast to a $10^{-6} - 0^{-5}$ in stark contrast to the Gaussian aperture. More importantly, one must consider the large depth of field (3 cm) of the grating surface. The inset of Fig. 2(a) shows the result of the Fresnel knife-edge diffraction [15] at 0.5 mm transverse distance from the edge for increasing propagation distances. This diffraction from best focus could impose a limit to the window partitioning of 10^{-3} , two orders larger than that of the imaging. Fig. 2(b) shows that the actual performance is better than expected from the Fresnel calculation though the uncertainty in experimental parameters precludes exact determination of the contrast floor. A 2 mm etalon produced a 10^{-3} reflection with 20 ps delay. Two filters, nominally specified to total OD 6, were positioned over the principle peak. The observed small peak, a factor 15 below the unfiltered etalon peak, corresponds to a total attenuation 7×10^{-5} . Near perfect positioning on the grating is possible, though another explanation might be the OPA angular acceptance, which would non-linearly select against the inferior diffracted beam quality. From the diffraction calculation, the phase front in the shadow region has 100 mr tilt resulting in Δk of ~ 100 mm $^{-1}$. Using the lesser OD, direct light energy transmits and peaks appear with roughly the same magnitude. A first reflection from the slide also appears at ~ 10 ps. Though we see success in improving single-window dynamic range the allusion to OPA non-linearity suggests future implementation in the pump line, where 10x attenuation would suffice for 10^3 variation in gain. The effect of the spatially selective filters on the pump gain could be calibrated using known full aperture densities in the signal line.

Finally, Fig. 3 presents measurement of the pulse contrast using the few-shot correlator and only full aperture optical densities in the signal path. The relative position of each window is corrected based on the glass thickness and delay line positioning. The peak at 50 ps results from a 5 mm etalon inserted in the input beam. The strength

of this reflection served as a calibration point for the most optically dense glass while the other densities were calibrated independently. The label "pump blocked" indicates the detection limit at 10^{-8} relative to the pulse peak due to signal beam scattering. The noise floor of each temporal window coincides with its smallest measurement. The few shot scan is referenced to a measurement made using a commercial scanning auto-correlator (Del Mar Photonics, San Diego) for which we have measured the dynamic range as better than 10^8 . Peaks at ± 30 ps correspond to reflections in the filter-wheel of the commercial device. Measurement between -50 to -20 ps with the few-shot system would require the addition of a hard aperture selecting the temporal window since at these negative delays, the contrast drops immediately to 10^{-7} . The peak at 75 ps falls below the dynamic range of the CCD and exemplifies the motivation for future implementation of window partitioning. There is some increased structure in the few-shot measurement, particularly at ± 100 ps which should not detract from use in many applications. In this case, the high repetition rate allowed optimizing alignment at each position to compensate for mis-alignments. Holding the position constant, five separate measurements showed maximum factor two variation. Implementation with low-repetition large amplifiers would require independent alignment fiducials and input energy monitoring.

4 Conclusions

This work addresses the need for high-dynamic range, few/single shot measurements of pulse contrast. Use of high-gain optical parametric amplification with a large pulse tilt results in $> 10^7$ dynamic range between single-shot windows of 50 ps with 250 μ J. There is good agreement with scanning measurement at the expense of a temporal resolution of few ps. The limit on dynamic range arises from scattering of the degenerate signal into the idler. Use of a raman medium (i.e. KGW crystal [16] or He gas [17]) might provide a work-around allowing achievement of the OPN limit. We have also explored use of optical densities which partition the CCD image and expand its dynamic range. In this case, the filters were placed in an imaging plane of the signal beam and the dynamic range increased by $> 10^3$. The analysis suggests that future implementation with such filters in the pump path would substantially improve the achievable single window dynamic range beyond the current work.

References

1. L. Yin, B. J. Albright, B. M. Hegelich, K. J. Bowers, K. A. Flippo, T. J. T. Kwan, and J. C. Fernández. Monoenergetic and gev ion acceleration from the laser breakout afterburner using ultrathin targets. *Physics of Plasmas*, 14(5):056706, 2007.
2. Ed Gerstner. Laser physics: Extreme light. *Nature*, 446:16, 2007.
3. G. Priebe, K.A. Janulewicz, V.I. Redkorechey, J. Tümler, and P.V. Nickles. Pulse shape measurement by a non-collinear third-order correlation technique. *Opt. Comm.*, 259:848, 2006.
4. N. V. Didenko, A. V. Konyashchenko, A. P. Lutsenko, and S. Y. Tenyakov. Contrast degradation in a chirped-pulse amplifier due to generation of prepulses by postpulses. *Opt. Express*, 16(5):3178–3190, 2008.
5. Christophe Dorrer, Jake Bromage, and J. D. Zuegel. High-dynamic-range single-shot cross-correlator based on an optical pulse replicator. *Opt. Express*, 16(18):13534–13544, 2008.
6. J. Collier, C. Hernandez-Gomez, R. Allott, C. Danson, and A. Hall. A single-shot third-order autocorrelator for pulse contrast and pulse shape measurements. *Laser and Particle Beams*, 19(19):231–235, 2001.
7. I. Jovanovic, C. Brown, C. Haefner, M. Shverdin, M. Tarannowski, and C.P.J. Barty. High-dynamic-range, 200-ps window, single-shot cross-correlator for ultrahigh intensity laser characterization. In *Conference on Lasers and Electro-Optics/Quantum Technologies Technical Digest (Optical Society of America, Washington, DC*, page JThD137, Washington, DC, 2007. Optical Society of America.
8. D. Javorková and V. Bagnoud. 60-db-dynamic-range short-pulse measurement from an 8-bit cmos camera. *Opt. Express*, 15(9):5439–5444, 2007.
9. Edwin J. Divall and Ian N. Ross. High dynamic range contrast measurements by use of an optical parametricamplifier correlator. *Opt. Lett.*, 29(19):2273–2275, 2004.
10. Amnon Yariv and Pochi Yeh. *Optical Waves in Crystals*. John Wiley & Sons, New York, 1984.
11. D. A. Kleinman. Theory of optical parametric noise. *Phys. Rev.*, 174(3):1027–1041, Oct 1968.
12. D. Marcuse. *Principles of Quantum Electronics*. Academic Press, Inc., Orlando, 1980.
13. Zsolt Bör, Béla Rácz, Gabor Szabó, Margit Hilbert, and H. A. Hazim. Femtosecond pulse front tilt caused by angular dispersion. *Optical Engineering*, 32:2501, 1993.

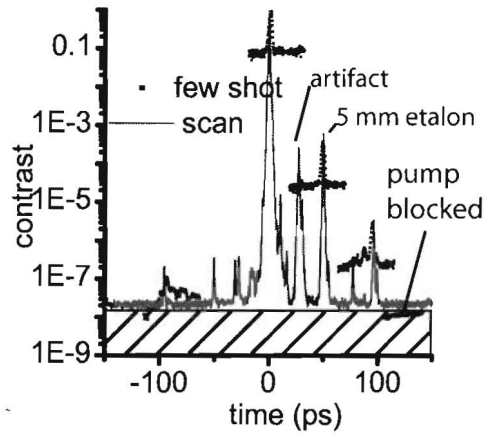


Fig. 3. Few-shot contrast measurement using full-aperture optical densities (black squares) and reference measurement using commercial scanning device (red line). Measurement between -50 to -20 ps would require a properly sized aperture on either the crystal or CCD. Hatched region corresponds to noise floor for few-shot device. SHAHdata-fig3.eps.

14. K. Iizuka. *Engineering Optics*. Springer-Verlag, Berlin, 1983.
15. Eugene Hecht. *Optics*. Addison-Wesley, Menlo Park, 1979.
16. Arkady Major, J. Stewart Aitchison, Peter W. E. Smith, Nigel Langford, and Allister I. Ferguson. Efficient raman shifting of high-energy picosecond pulses into the eye-safe 1.5- μ m spectral region by use of a kgd(wo4)2 crystal. *Opt. Lett.*, 30(4):421–423, 2005.
17. V. Krylov, A. Rebane, O. Ollikainen, D. Erni, Urs P. Wild, V. Bespalov, and D. Staselko. Stimulated raman scattering in hydrogen by frequency-doubled amplified femtosecond ti:sapphire laser pulses. *Opt. Lett.*, 21(6):381, 1996.